Philip S. Light, Ashby P. Hilton, Richard T. White, Christopher Perrella, James D. Anstie, John G. Hartnett, Giorgio Santarelli and Andre N. Luiten

Bidirectional microwave and optical signal dissemination

Optics Letters, 2016; 41(5):1014-1017

Bidirectional Microwave and Optical Signal Dissemination

Philip S Light[1,*], **Ashby P Hilton**[1], **Richard T White**[1], **Christopher Perrella**[1], **James D Anstie**[1], **John G Hartnett**[1], **Giorgio Santarelli**[2], and **Andre N Luiten**[1]

[1] *Institute for Photonics and Advanced Sensing (IPAS) and School of Physical Sciences, The University of Adelaide, Adelaide, SA 5005, Australia*
[2] *Laboratoire Photonique, Numérique et Nanosciences, UMR 5298, Institut d'Optique Graduate School, CNRS and Université de Bordeaux, 1, Rue F. Mitterrand, 33400 Talence, France*
[*] *Corresponding author: philip.light@adelaide.edu.au*

Compiled January 11, 2016

We describe a technique to disseminate highly stable microwave and optical signals from physically separated frequency standards to multiple locations. We demonstrate our technique by transferring the frequency stability performance of a microwave frequency reference to the repetition-rate stability of an optical frequency comb in a different location. The stabilized optical frequency comb becomes available in both locations for measurements of both optical and microwave signals. We show a microwave frequency stability of 4×10^{-15} in both locations for integration times beyond 100 s. The control system uses only a standard Ethernet connection.

OCIS codes:

http://dx.doi.org/10.1364/ao.XX.XXXXxXX

The drive for accurate and precise measurements at numerous locations has motivated the development of sophisticated frequency dissemination techniques over recent years [1, 2]. Optical fiber links have shown potential to transfer frequency with outstanding accuracy and stability. Several approaches involving both radio-frequency and microwave intensity modulated optical carriers [3], frequency mixing [4], pure optical phase [5, 6] and even femtosecond frequency combs schemes [7, 8] have been implemented on fiber links ranging from a few km up to the continental scale. Frequency transfer over optical fiber to multiple endpoints has also been demonstrated [9–14]. In this paper, we implement an original approach for simultaneous transfer of optical and microwave frequency stability.

We consider here the situation where there is a physical separation between the reference frequency standard and the apparatus used to disseminate that reference signal. Our technique allows the full dissemination of the reference signal. In our particular implementation this reference frequency standard is in the microwave domain and our approach also translates this into the optical domain so that its full performance is now available at any fiber-connected location in both the optical and microwave domain. In one laboratory, an optical frequency comb provides a means to measure optical signals, as well as microwave signals by derivation of the microwave frequency from the comb's repetition rate. Frequency combs are usually stabilized to a high-performance optical frequency standard to suppress the instability into the 10^{-14} range or better [15]. However, in many laboratories such high-performance optical standard is not available, although there may be a nearby high-performance microwave standard (e.g. hydrogen maser, Cs or Rb clock). Our experiment considers exactly this situation, allowing stabilization of the optical frequency comb to that microwave frequency standard. Furthermore, our technique results in the stabilized frequency comb signals being available in both locations as well as the microwave signals. This allows precision measurements of optical and microwave signals in both locations with performance limited only by that of the frequency standard itself.

Our system consists of a cavity-stabilized optical frequency comb, to which we transfer the long-term (>10 s) stability of a cryogenic sapphire oscillator (CSO) microwave reference. The optical frequency comb and microwave CSO were physically separated, being located in laboratories in different buildings on the same campus, referred to as 'Lab A' and 'Lab B' respectively. The buildings were linked by a 1.6 km optical fiber, with 6 dB one-way loss. The arrangement that disseminates the optical and microwave signals in both directions between the two locations is illustrated schematically in Fig. 1.

The 1560 nm (∼50 nm bandwidth) optical frequency comb (OFC) (Menlo Systems FC1500) has a repetition rate of ∼250 MHz, tuneable over a 2 MHz. The carrier envelope offset frequency (CEO) of the comb was stabilized at 20 MHz. The repetition rate of the comb was controlled by phase-locking (via feedback to the comb's intracavity EOM with ∼1 MHz bandwidth) a selected comb mode to a cavity-stabilized 1560 nm reference laser (NKT Adjustik E15 fiber laser), such that the repetition rate was defined by $\omega_n = n\omega_{rep} + \omega_{ceo}$, where n is index of the selected comb mode. The exact repetition rate could be coarsely tuned by choosing a particular value of n, and fine tuned by shifting the frequency of the reference laser using an acousto-optic modulator (AOM1 in Fig. 1). The reference laser was locked to a low-finesse Fabry-Perot optical cavity to provide 10^{-13} frequency stability at 1 s integration time. Figure 3

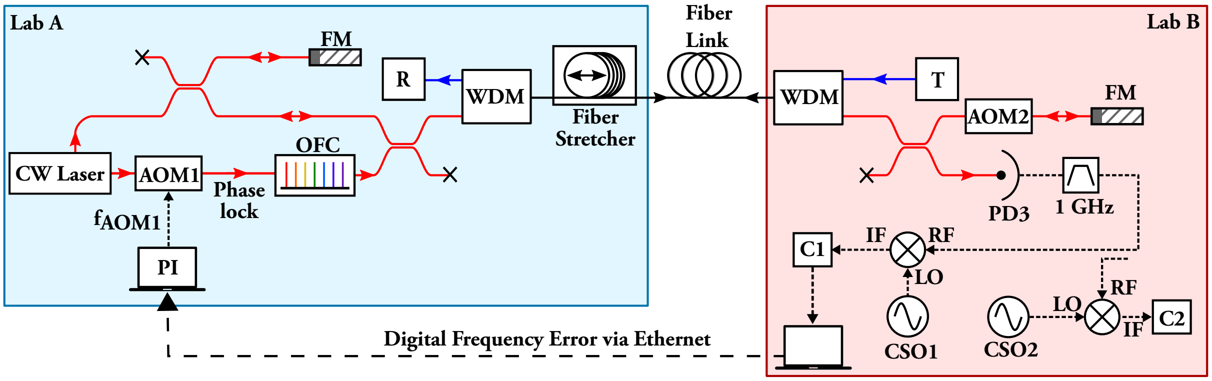

Fig. 1. Schematic diagram of dissemination technique, showing fiber optic links (solid lines) and microwave/RF electrical paths (dashed lines). The 1560 nm optical frequency comb and 1560 nm CW reference laser paths are shown in red, while the 1310 nm amplitude modulated laser path is shown in blue. OFC: optical frequency comb. All optical components are fiber coupled, where FM refers to the Faraday mirrors, WDM refers to the wavelength multiplexers, $PD2$ is a photodiode, and AOM_1 and AOM_2 are acousto-optic modulators. The devices labeled **T** and **R** are a microwave to optical AM transmitter, and an AM optical to microwave receiver, respectively. Devices C1 and C2 are in-loop and out of loop frequency counters.

shows the stability of the OFC repetition rate in this configuration (black diamonds), which was limited by the stability of the optical cavity.

The remote microwave frequency standard was a cryogenic sapphire oscillator (CSO), operating at a fundamental frequency of 11.2 GHz. The CSO consists of a cylindrical sapphire crystal resonator 51 mm in diameter and 30 mm high in which a whispering gallery microwave mode is excited. The mode bandwidth was 11.2 Hz, corresponding to a loaded Q-factor of

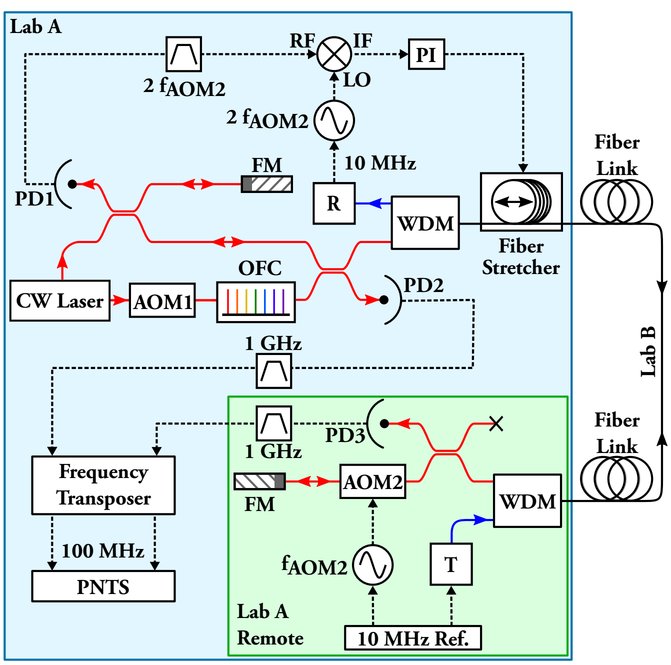

Fig. 2. Schematic diagram of the setup used to stabilize fiber-length and verify repetition-rate transfer performance over a full round-trip between Lab A and Lab B. Both 'local' and 'remote' ends of the optical fiber are located in Lab A. PNTS: Symmetricom phase-noise test set; $PD1$, $PD2$ and $PD3$: photodiodes. Blue lines highlight the transfer of the 10 MHz reference signal at 1310 nm.

1×10^9 [16]. A closed-cycle cryostat maintained the temperature of the sapphire near 4 K, the frequency-temperature turning point of the chosen mode. A 1 GHz signal was derived from the fundamental CSO output using a frequency synthesizer similar to that described in [17]. The frequency stability of this 1 GHz output, derived through comparison of two independent oscillators, is shown in Fig. 3 (green dashed line).

In order to compare the repetition rate of the optical frequency comb to the CSO reference, a comparison was made between the 1 GHz output of the CSO, and fourth harmonic of the OFC repetition rate. This harmonic at ∼1 GHz was chosen due its proximity to the synthesized CSO signal.

In order to stabilize the OFC repetition rate against the CSO, 6 mW of comb light was sent to Lab B over the optical fiber link, where a photodiode (PD3) detected the repetition rate of the comb and its harmonics. The fourth-harmonic of the repetition rate was filtered out and compared with the CSO output. The comb repetition-rate was tuned to produce a ∼95 kHz offset from the CSO 1 GHz signal, which was then measured using a frequency counter (Agilent 53131A). The measured beat frequency was recorded by software on a PC, and compared to a digital frequency set-point.

In order to correct the OFC repetition rate, the difference between the set-point and measured frequency was sent to a PC in Lab A via an Ethernet network connection, which we term "carrier pigeon" stabilization, reflecting its relatively low bandwidth. The local PC then applied a corresponding optical frequency correction (Eqn. 1) to the pre-stabilized laser by changing the frequency shift provided by AOM1:

$$\Delta f_{AOM1} = \Delta \nu_{opt} = (f_{beat} - f_{set}) \frac{\nu_{opt}}{\nu_{comp}} \qquad \textbf{(1)}$$

where ν_{opt} is the optical frequency of the OFC (192 THz), ν_{comp} is the frequency at which the comparison between OFC and CSO was made 1 GHz, f_{beat} is the measured frequency offset between repetition rate and CSO output signal, and f_{set} is the digital set-point frequency. This in turn provided a correction to the repetition rate of the optical frequency comb via the phase-lock between the pre-stabilized laser and nearest comb mode. This software-based servo was configured as a pure integrator.

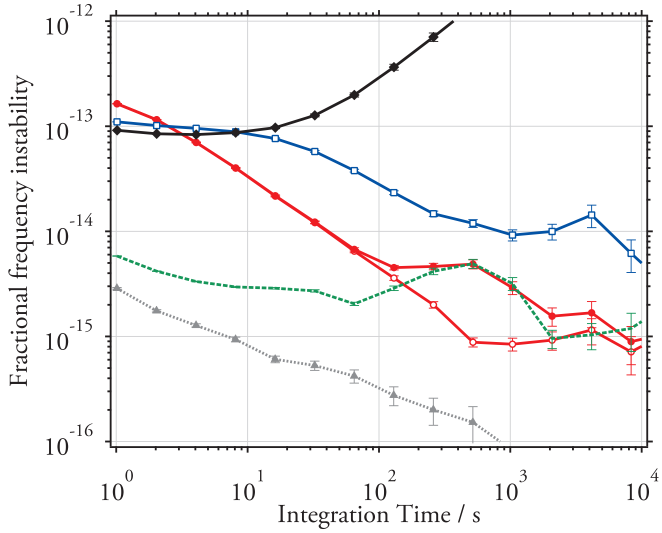

Fig. 3. Performance of the bidirectional stability transfer technique, illustrated by fractional frequency of the optical frequency comb repetition rate: unstabilized comb (black, diamonds); stabilized with integrator time constants of 10 s (blue, open squares) and 1.3 s (red, open circles); independent measurement of performance (red, filled circles); derived performance of CSO standards (see main text) (green, dashed); repetition rate measurement floor (gray, triangles). In all cases the phase-lock between cavity-stabilized laser and the optical frequency comb is engaged.

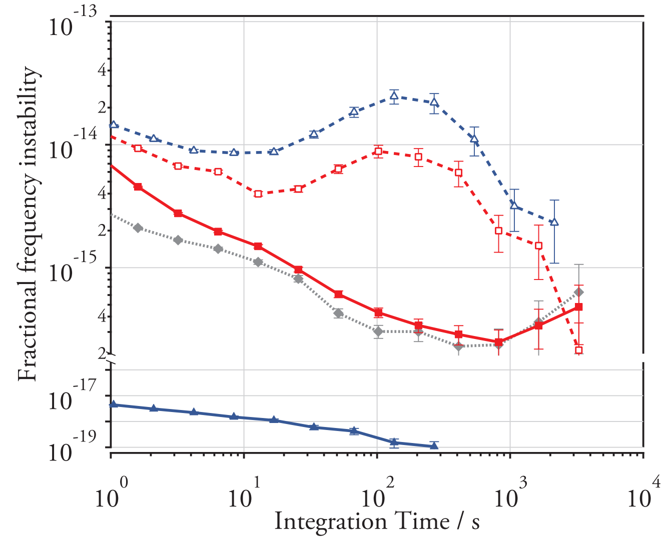

Fig. 4. Optical fiber transfer performance over 3.2 km link: comb repetition-rate stability (at 1 GHz) with length unstabilized (red, open squares) and stabilized (red, filled squares); repetition-rate measurement floor (gray, diamonds); optical stability (at 192 THz) with length unstabilized (blue, open triangles) and stabilized (blue, filled triangles).

An out-of-loop measurement of OFC repetition-rate performance was made with an independent CSO also located in Lab B. In order to transfer the full stability of the CSO microwave reference to the OFC located in Lab A, at integration times beyond 100 s it was necessary to stabilize the length of the optical fiber link between buildings. A standard fiber-length stabilization technique was used [1], whereby an unbalanced Michelson interferometer detected fiber length fluctuations. The prestabilized reference laser was coupled through the optical fiber link, and frequency shifted by 80 MHz by an AOM at the remote end (*AOM*2 in Fig. 2). A Faraday mirror reflected this light back through the fiber link, and the returned signal (frequency shifted by 160 MHz) combined with the reflection from a local reference arm formed a beat note that was detected on a photodiode (PD1). This signal was mixed with a 160 MHz local oscillator to generate a fiber-stabilization error signal. This signal was passed to a PI filter (New Focus LB1005) with the correction signal of the length fluctuations sent to a piezoelectric fiber stretcher (with 1 kHz bandwidth, and 1.4 mm range) to correct fiber length fluctuations. Importantly, the *AOM*2 and demodulation frequencies shared a common time-base, which was distributed over the fiber link using AM modulation at 1310 nm as shown in Fig. 2. We note that it would be possible to eliminate this 1310 nm laser by deriving the timebase through division of the repetition rate signal in both locations.

In order to verify the transfer performance over the length-stabilized optical fiber link, we created a fiber loop on two independent fibers from Lab A to Lab B and back to Lab A (total length 3.2 km), such that a direct comparison could be made between the local comb launched into the fiber link, and the comb after passing through the fiber loop (see Fig. 2). This measurement was performed using custom electronics [18] to mix the 1 GHz beat signals down to 100 MHz with minimal phase-noise deterioration, such that the phase-noise (and thus frequency stability) could be measured using a Symmetricom 5125A phase-noise test set. This measurement was performed across the full fiber loop. We expect performance on the one-way 1.6 km fiber link used for the bidirectional microwave and optical transfer dissemination to be equal or better than that measured for the 3.2 km round-trip.

The performance of the transfer technique is summarized in Fig. 3. The stability of the frequency comb repetition rate, before stabilization to the microwave reference, is shown in black, with a stability of 1×10^{-13} at 1 s integration time, which deteriorates at longer integration times due to the thermal drifts in the optical frequency reference.

With the "carrier-pigeon" servo engaged, we see that the microwave performance of the CSO is transferred to the repetition rate of the frequency comb. This is illustrated in the figure for integration time constants of 1.3 s (red open circles) and 10 s (blue open squares). For the 1.3 s time-constant, an in-loop repetition rate stability of 9×10^{-16} is reached after an integration time of 500 s. The out-of-loop measurement against an independent CSO for this case is also shown on the graph (red filled circles); for integration times between 100 s and 2000 s we see the limit of the CSO performance over these timescales, rather than a limitation of this stabilization technique. CSO performance can be derived from the difference between the frequencies measured at the two counters, i.e. the comparison of the comb repetition rate with each of the two CSOs. This is shown by the dashed green curve in Fig. 3.

As noted above, it is important that the optical fiber link length is stabilized so that the repetition rate stability of the OFC in Lab A is identical to that of the repetition rate stability of the OFC transferred to Lab B. This is illustrated in Fig. 4, which shows the effect of transferring the OFC over the 3.2 km fiber round-trip described above. The red dashed and solid curves show OFC repetition-rate transfer stability (measured at 1 GHz) for length-unstabilized and length-stabilized fiber links respectively. At 100 s integration time, the length-unstabilized fiber contributes 9×10^{-15} fractional frequency instability; this is higher than the 5×10^{-15} achieved by the carrier-pigeon technique, and thus limits the repetition rate stability in Lab A. Locking the fiber-length significantly reduces the fiber-induced stability to a level close to the measurement noise floor (grey curve), contribution only 4×10^{-16} at 100 s. The noise floor was determined by splitting the OFC in Lab A directly into two photodiodes, and performing a comparison of the measured repetition rates. For completeness, Fig. 4 also shows optical transfer stability, by blue dashed and solid curves, for unstabilized and stabilized fiber link length respectively. One would expect that the transferred microwave signal performance (red-dashed curve) and optical performance (blue-dashed curve) to be correlated when unstabilized. The factor of two difference we see here we put down to the measurements occurring at different times.

The residual noise of the "carrier-pigeon" stabilized links is set by the gain of the loop. For 1.3 s time-constant we can transfer the full stability of the CSO for integration times longer than 100 s. However, for 10 s time-constant, there is insufficient gain even at 10^4 s to transfer the full microwave stability, due to the large frequency drift of the unstabilized repetition rate (black curve on Fig. 3, with gradient τ beyond 100 s. Minor degradation of the 1 s performance was experienced due to the low carrier-pigeon sampling rate (from Nyquist's Theorem, a counter gate time of 1 s yields useful information at integration times $>$2 s and adds noise at shorter integration times).

There is a necessary trade-off between the potential gain of the "carrier pigeon" system and the noise-floor, which is set by the characteristics of the frequency counter. In order to measure the 95 kHz frequency to sufficient precision, we selected a 1 s gate time. This provides the noise floor indicated by the gray triangles on figure 3, which represents the counter noise-floor in comparing the comb repetition rate and CSO output signals. Using a shorter gate time, allowing increased gain, would mean the counter, rather than the CSO, would limit the achievable stability. We note that use of a different frequency counter (e.g. Agilent 53132A) would lower this floor by an order-of-magnitude and allow an equivalent increase in gain by allowing shorter counter gate times.

In conclusion, we have demonstrated the bidirectional transfer of a stable microwave frequency from a reference in one location to the repetition rate of an optical frequency comb in a second location, as well as the simultaneous transfer of the stabilized comb to the microwave oscillator laboratory. The full performance of the CSO is transferred to the OFC for integration times beyond 100 s, where the repetition rate stability is better than 5×10^{-15}. The correction to the frequency comb's repetition rate is achieved through a low-bandwidth network-based servo system (affectionately called carrier-pigeon control) that is simple, reliable and flexible.

This research is supported by the Australian Research Council through grants DE120102028 and FT0990301, and by the South Australian Government through the Premier's Science and Research Fund.

REFERENCES

1. L. Ma, P. Junger, J. Ye, and J. Hall, Optics Letters **19**, 1777 (1994).
2. S. M. Foreman, K. W. Holman, D. D. Hudson, D. J. Jones, and J. Ye, Review of Scientific Instruments **78** (2007).
3. O. Lopez, A. Amy-Klein, M. Lours, C. Chardonnet, and G. Santarelli, Applied Physics B-Lasers and Optics **98**, 723 (2010).
4. Y. He, B. J. Orr, K. G. H. Baldwin, M. J. Wouters, A. N. Luiten, G. Aben, and R. B. Warrington, Optics Express **21**, 18754 (2013).
5. K. Predehl, G. Grosche, S. M. F. Raupach, S. Droste, O. Terra, J. Alnis, T. Legero, T. W. Haensch, T. Udem, R. Holzwarth, and H. Schnatz, Science **336**, 441 (2012).
6. O. Lopez, F. Kefelian, H. Jiang, A. Haboucha, A. Bercy, F. Stefani, B. Chanteau, A. Kanj, D. Rovera, J. Achkar, C. Chardonnet, P.-E. Pottie, A. Amy-Klein, and G. Santarelli, Comptes Rendus Physique **16**, 531 (2015).
7. G. Marra, H. S. Margolis, and D. J. Richardson, Optics Express **20**, 1775 (2012).
8. S. M. F. Raupach, T. Legero, C. Grebing, C. Hagemann, T. Kessler, A. Koczwara, B. Lipphardt, M. Misera, H. Schnatz, G. Grosche, and U. Sterr, Applied Physics B-Lasers and Optics **110**, 465 (2013).
9. C. Gao, B. Wang, W. L. Chen, Y. Bai, J. Miao, X. Zhu, T. C. Li, and L. J. Wang, Optics Letters **37**, 4690 (2012).
10. S. W. Schediwy, D. Gozzard, K. G. H. Baldwin, B. J. Orr, R. B. Warrington, G. Aben, and A. N. Luiten, Optics Letters **38**, 2893 (2013).
11. P. Krehlik, L. Sliwczynski, L. Buczek, and M. Lipinski, IEEE Transactions on Ultrasonics, Ferroelectrics and Frequency Control **60**, 1804 (2013).
12. A. Bercy, S. Guellati-Khelifa, F. Stefani, G. Santarelli, C. Chardonnet, P.-E. Pottie, O. Lopez, and A. Amy-Klein, Journal of the Optical Society of America B-Optical Physics **31**, 678 (2014).
13. G. Grosche, Optics Letters **39**, 2545 (2014).
14. Y. Bai, B. Wang, C. Gao, J. Miao, X. Zhu, and L. Wang, Chinese Optics Letters **13** (2015).
15. S. Häfner, S. Falke, C. Grebing, S. Vogt, T. Legero, M. Merimaa, C. Lisdat, and U. Sterr, Optics Letters **40**, 2112 (2015).
16. J. Hartnett, N. Nand, and C. Lu, Appl. Phys. Lett. **100**, 183501 (2012).
17. N. R. Nand, J. G. Hartnett, E. N. Ivanov, and G. Santarelli, IEEE Transactions on Microwave Theory and Techniques **59**, 2978 (2011).
18. J. G. Hartnett, S. R. Parker, and E. N. Ivanov, Electronics Letters **49**, 947 (2013).

REFERENCES

1. L. Ma, P. Junger, J. Ye, and J. Hall, "Delivering the same optical frequency at 2 places - Accurate cancellation of phase noise introduced by an optical-fiber or other time-varying path," Optics Letters **19**, 1777 (1994).
2. S. M. Foreman, K. W. Holman, D. D. Hudson, D. J. Jones, and J. Ye, "Remote transfer of ultrastable frequency references via fiber networks," Review of Scientific Instruments **78** (2007).
3. O. Lopez, A. Amy-Klein, M. Lours, C. Chardonnet, and G. Santarelli, "High-resolution microwave frequency dissemination on an 86-km urban optical link," Applied Physics B-Lasers and Optics **98**, 723 (2010).
4. Y. He, B. J. Orr, K. G. H. Baldwin, M. J. Wouters, A. N. Luiten, G. Aben, and R. B. Warrington, "Stable radio-frequency transfer over optical fiber by phase-conjugate frequency mixing," Optics Express **21**, 18754 (2013).
5. K. Predehl, G. Grosche, S. M. F. Raupach, S. Droste, O. Terra, J. Alnis, T. Legero, T. W. Haensch, T. Udem, R. Holzwarth, and H. Schnatz, "A 920-Kilometer Optical Fiber Link for Frequency Metrology at the 19th Decimal Place," Science **336**, 441 (2012).
6. O. Lopez, F. Kefelian, H. Jiang, A. Haboucha, A. Bercy, F. Stefani, B. Chanteau, A. Kanj, D. Rovera, J. Achkar, C. Chardonnet, P.-E. Pottie, A. Amy-Klein, and G. Santarelli, "Frequency and time transfer for metrology and beyond using telecommunication network fibres," Comptes Rendus Physique **16**, 531 (2015).
7. G. Marra, H. S. Margolis, and D. J. Richardson, "Dissemination of an optical frequency comb over fiber with 3 x 10(-18) fractional accuracy," Optics Express **20**, 1775 (2012).
8. S. M. F. Raupach, T. Legero, C. Grebing, C. Hagemann, T. Kessler, A. Koczwara, B. Lipphardt, M. Misera, H. Schnatz, G. Grosche, and U. Sterr, "Subhertz-linewidth infrared frequency source with a long-term instability below 5 x 10(-15)," Applied Physics B-Lasers and Optics **110**, 465 (2013).
9. C. Gao, B. Wang, W. L. Chen, Y. Bai, J. Miao, X. Zhu, T. C. Li, and L. J. Wang, "Fiber-based multiple-access ultrastable frequency dissemination," Optics Letters **37**, 4690 (2012).
10. S. W. Schediwy, D. Gozzard, K. G. H. Baldwin, B. J. Orr, R. B. Warrington, G. Aben, and A. N. Luiten, "High-precision optical-frequency dissemination on branching optical-fiber networks," Optics Letters **38**, 2893 (2013).
11. P. Krehlik, L. Sliwczynski, L. Buczek, and M. Lipinski, "Multipoint Dissemination of RF Frequency in Fiber Optic Link With Stabilized Propagation Delay," IEEE Transactions on Ultrasonics, Ferroelectrics and Frequency Control **60**, 1804 (2013).
12. A. Bercy, S. Guellati-Khelifa, F. Stefani, G. Santarelli, C. Chardonnet, P.-E. Pottie, O. Lopez, and A. Amy-Klein, "In-line extraction of an ultrastable frequency signal over an optical fiber link," Journal of the Optical Society of America B-Optical Physics **31**, 678 (2014).
13. G. Grosche, "Eavesdropping time and frequency: phase noise cancellation along a time-varying path, such as an optical fiber," Optics Letters **39**, 2545 (2014).
14. Y. Bai, B. Wang, C. Gao, J. Miao, X. Zhu, and L. Wang, "Fiber-based radio frequency dissemination for branching networks with passive phase-noise cancelation," Chinese Optics Letters **13** (2015).
15. S. Häfner, S. Falke, C. Grebing, S. Vogt, T. Legero, M. Merimaa, C. Lisdat, and U. Sterr, "8x10ˆ-17 fractional laser frequency instability with a long room-temperature cavity," Optics Letters **40**, 2112 (2015).
16. J. Hartnett, N. Nand, and C. Lu, "Ultra-low-phase-noise cryocooled microwave dielectric-sapphire-resonator oscillators," Appl. Phys. Lett. **100**, 183501 (2012).
17. N. R. Nand, J. G. Hartnett, E. N. Ivanov, and G. Santarelli, "Ultra-Stable Very-Low Phase-Noise Signal Source for Very Long Baseline Interferometry Using a Cryocooled Sapphire Oscillator," IEEE Transactions on Microwave Theory and Techniques **59**, 2978 (2011).
18. J. G. Hartnett, S. R. Parker, and E. N. Ivanov, "Frequency transposing measurement technique for oscillator comparisons," Electronics Letters **49**, 947 (2013).